Electromagnetic structure of the ρ meson in the light-front quark model

Ho-Meoyng Choi[1] and Chueng-Ryong Ji[2]

[1]*Department of Physics, Kyungpook National University, Daegu, 702-701 Korea*
[2]*Department of Physics, North Carolina State University, Raleigh, North Carolina 27695-8202, USA*

We investigate the elastic form factors of the ρ meson in the light-front quark model (LFQM). With the phenomenologically accessible meson vertices including the one obtained by the Melosh transformation frequently used in the LFQM, we find that only the helicity $0 \rightarrow 0$ matrix element of the plus current receives the zero-mode contribution. We quantify the zero-mode contribution in the helicity $0 \rightarrow 0$ amplitude using the angular condition of spin-1 system. After taking care of the zero-mode issue, we obtain the magnetic (μ) and quadrupole (Q) moments of the ρ meson as $\mu = 1.92$ and $Q = 0.43$, respectively, in the LFQM consistent with the Melosh transformation and compare our results with other available theoretical predictions.

I. INTRODUCTION

In the past few years, there has been much theoretical effort [1–9] to study the so-called "zero-mode" [10–15] contribution to the elastic and weak form factors for spin-0 and spin-1 systems in light-front dynamics (LFD). The zero mode is closely related to the off-diagonal elements in the Fock state expansion of the current matrix. In particular, the zero-mode contribution to the form factor $F(q^2)$ can be characterized by the nonvanishing contribution from the off-diagonal elements in the $q^+ \rightarrow 0$ limit, where q^+ is the longitudinal component of the momentum transfer q ($q^{\pm} = q^0 \pm q^3$, $q^2 = q^+ q^- - \mathbf{q}_{\perp}^2$). In the absence of zero mode, however, the hadron form factors can be expressed as the convolution of the initial and final LF wave functions; namely, the physical result can be obtained by taking into account only the valence contribution or the diagonal elements in the Fock state expansion.

In this work, we analyze the zero-mode contribution to the elastic form factors of the ρ meson using the LF constituent quark model (or LFQM for short) [16–22], which has been quite successful in predicting various electroweak properties of light and heavy mesons compared to the available data. In our previous LFD analysis [6] of spin-1 electromagnetic form factors, we have shown that the zero-mode complication can exist even in the matrix element of the plus component of the current. Using a covariant model of the spin-1 system with the polarization vectors obtained from the LF gauge ($\epsilon_{\pm}^+ = 0$), we found that only the helicity zero-to-zero amplitude, i.e., $(h', h) = (0, 0)$, can be contaminated by the zero-mode contribution. However, our conclusion in [6] was based on the use of a rather simple vector meson vertex $\Gamma^{\mu} = \gamma^{\mu}$. The aim of the present work is to explore our findings in the more phenomenologically accessible ρ meson vertex [see Eq. (12)]. This includes the case of the ρ meson vertex obtained by the Melosh transformation frequently used in the LFQM.

Recently, Jaus [3,8] proposed a covariant light-front approach that develops a way of including the zero-mode contribution and removing spurious form factors proportional to the lightlike vector $\omega^{\mu} = (1, 0, 0, -1)$. Using the LFQM vector meson vertex that we include in this work, the author in [8] concluded the existence of a zero mode in the form factor $F_2(Q^2)$ of a spin-1 meson. Although his calculation was performed in a covariant way not using the helicity components, the form factor F_2 is related to the matrix element of the $(h', h) = (+, 0)$ component of the current [see Eq. (2.6) in [8]] as well as the $(h', h) = (0, 0)$ component. Thus, according to his formulation, both helicity $(+, 0)$ and $(0, 0)$ amplitudes receive the zero-mode contribution [23]. As we show in the present work, we do not agree with this result but find the zero-mode contribution only in the helicity $(h', h) = (0, 0)$ amplitude. However, Jaus and we agree [23] that there is a subtle difference between his (ω-dependent) formulation and our formulation (not involving ω as a variable) which leads to different conclusions regarding the effect of the zero modes. It may call for a further clarification whether the ω-dependent formulation adds the more complication in the effect of zero modes. We stress that our formulation should be intrinsically distinguished from the formulation involving ω, since our formulation involves neither ω nor any unphysical form factor. Our finding of zero mode only in the helicity $(0, 0)$ amplitude is quite significant in the LFQM phenomenology because the absence of the zero-mode contamination in the helicity $(+, 0)$ amplitude can give a tremendous benefit in making reliable predictions on the spin-1 observables as we present in the example of the ρ meson.

The paper is organized as follows. In Sec. II, we present the Lorentz-invariant electromagnetic form factors and the kinematics for the reference frames used in our analysis. We also discuss the LF helicity basis, the angular condition for spin-1 systems, and the two particular prescriptions used in extracting the physical form factors. In Sec. III, we present our LF calculation varying the vector

meson vertex. We employ both the manifestly covariant model vertex (beyond the simple model of $\Gamma^\mu = \gamma^\mu$) and the LFQM vertex consistent with the Melosh transformation. We discuss the LF valence and the nonvalence contributions using a plus component of the current and show that only the helicity zero-to-zero amplitude receives zero-mode contribution for the employed meson vertices. In Sec. IV, we present our numerical results for the physical quantities of the ρ meson using the LFQM and compare our results with other available theoretical predictions. Conclusions follow in Sec. V. In the Appendix, we summarize our results of the trace calculations for various helicity components used in our form factor calculations.

II. ELECTROMAGNETIC STRUCTURE OF SPIN-1 SYSTEMS

The Lorentz-invariant electromagnetic form factors $F_i(i = 1, 2, 3)$ for a spin-1 particle are defined [24] by the matrix elements of the current J^μ between the initial $|P, h\rangle$ (momentum P and helicity h) and the final $|P', h'\rangle$ eigenstates as follows:

$$\langle P', h'|J^\mu|P, h\rangle = -\epsilon_{h'}^* \cdot \epsilon_h (P + P')^\mu F_1(Q^2) + (\epsilon_h^\mu q \cdot \epsilon_{h'}^*$$
$$- \epsilon_{h'}^{*\mu} q \cdot \epsilon_h) F_2(Q^2) + \frac{(\epsilon_{h'}^* \cdot q)(\epsilon_h \cdot q)}{2M_v^2}$$
$$\times (P + P')^\mu F_3(Q^2), \qquad (1)$$

where $q = P' - P$ and $\epsilon_h[\epsilon_{h'}]$ is the polarization vector of the initial [final] meson with the physical mass M_v.

We analyze the matrix elements in the Breit frame ($q^+ = 0$, $q_y = 0$, $q_x = Q$, and $\mathbf{P}_\perp = -\mathbf{P}'_\perp$) defined by [18,20,25–28]

$$q^\mu = (0, 0, Q, 0),$$
$$P^\mu = (M_v\sqrt{1 + \kappa}, M_v\sqrt{1 + \kappa}, -Q/2, 0), \qquad (2)$$
$$P'^\mu = (M_v\sqrt{1 + \kappa}, M_v\sqrt{1 + \kappa}, Q/2, 0),$$

where $\kappa = Q^2/4M_v^2$ is the kinematic factor. Here, we use the notation $p^\mu = (p^+, p^-, p^1, p^2)$ and the metric convention $p^2 = p^+ p^- - \mathbf{p}_\perp^2$ with $p^\pm = p^0 \pm p^3$.

Following the Bjorken-Drell convention [29], we work with the circular polarization and spin projection $h = \pm = \uparrow\downarrow$. With $\epsilon^+(p, \pm) = 0$ from the LF gauge [1], the initial and final transverse ($h = \pm$) and longitudinal ($h = 0$) polarization vectors in the Breit frame are given by

$$\epsilon^\mu(P, \pm) = \frac{\mp 1}{\sqrt{2}}\left(0, \frac{-Q}{P^+}, 1, \pm i\right),$$
$$\epsilon^\mu(P, 0) = \frac{1}{M_v}\left(P^+, \frac{-M_v^2 + Q^2/4}{P^+}, \frac{-Q}{2}, 0\right),$$
$$\epsilon^\mu(P', \pm) = \frac{\mp 1}{\sqrt{2}}\left(0, \frac{Q}{P^+}, 1, \pm i\right),$$
$$\epsilon^\mu(P', 0) = \frac{1}{M_v}\left(P^+, \frac{-M_v^2 + Q^2/4}{P^+}, \frac{Q}{2}, 0\right).$$

$$(3)$$

The covariant form factors of a spin-1 hadron in Eq. (1) can be determined using only the plus component of the current, $I_{h'h}^+(0) \equiv \langle P', h'|J^+|P, h\rangle$. As one can see from Eq. (1), while there are only three independent (invariant) form factors, nine elements of $I_{h'h}^+(0)$ can be assigned to the current operator. However, since the current matrix elements $I_{h'h}^+(0)$ must be constrained by the invariance under the LF parity and the LF time reversal, one can reduce the independent matrix elements of the current down to four, e.g., I_{++}^+, I_{+-}^+, I_{+0}^+, and I_{00}^+ [18,20,25–27,30]. The angular momentum conservation requires an additional constraint on the current operator, which yields the so-called "angular condition" $\Delta(Q^2)$ given by [25]

$$\Delta(Q^2) = (1 + 2\kappa)I_{++}^+ + I_{+-}^+ - \sqrt{8\kappa}I_{+0}^+ - I_{00}^+ = 0. \quad (4)$$

Because of the angular condition, only three helicity amplitudes are independent as expected from the three physical form factors. However, the relations between the physical form factors and the matrix elements $I_{h'h}^+$ are not uniquely determined because the number of helicity amplitudes is larger than that of physical form factors. For example, Grach and Kondratyuk (GK) [25] used $(h', h) = (+, +), (+, -)$, and $(+, 0)$ as one of their choices for the matrix elements. On the other hand, Brodsky and Hiller (BH) [27] used $(0, 0), (+, 0)$, and $(+, -)$ amplitudes considering that the $(0,0)$ component gives the most dominant contribution in the high momentum perturbative QCD (PQCD) region. Chung, Coester, Keister, and Polyzou [26] involved all helicity states, i.e., $(+, +)$, $(0, 0), (+, 0)$, and $(+, -)$. Among various choices, we present GK and BH prescriptions for the comparison purpose in this work. We note that, much earlier than the present work, Ref. [31] presented most of the available sets of choices for the matrix elements using the ω-dependent formulation and Ref. [32] presented the covariant calculation supporting the GK prescription with an effort to point out the role of the nonvalence contribution in LFD. In practical computation, instead of calculating the Lorentz-invariant form factors $F_i(Q^2)$, the physical charge (G_C), magnetic (G_M), and quadrupole (G_Q) form factors are often used. The relations between

F's and G's are given by

$$G_C = F_1 + \frac{2}{3}\kappa G_Q, \qquad G_M = -F_2,$$
$$G_Q = F_1 + F_2 + (1 + \kappa)F_3. \qquad (5)$$

The physical form factors (G_C, G_M, and G_Q) in terms of the matrix elements $I^+_{h'h}$ for GK and BH prescriptions are given by

$$G_C^{\text{GK}} = \frac{1}{2P^+}\left[\frac{(3-2\kappa)}{3}I^+_{++} + \frac{4\kappa}{3}\frac{I^+_{+0}}{\sqrt{2\kappa}} + \frac{1}{3}I^+_{+-}\right],$$
$$G_M^{\text{GK}} = \frac{2}{2P^+}\left[I^+_{++} - \frac{1}{\sqrt{2\kappa}}I^+_{+0}\right], \qquad (6)$$
$$G_Q^{\text{GK}} = \frac{1}{2P^+}\left[-I^+_{++} + 2\frac{I^+_{+0}}{\sqrt{2\kappa}} - \frac{I^+_{+-}}{\kappa}\right],$$

and

$$G_C^{\text{BH}} = \frac{1}{2P^+(1+2\kappa)}\left[\frac{3-2\kappa}{3}I^+_{00} + \frac{16}{3}\kappa\frac{I^+_{+0}}{\sqrt{2\kappa}}\right.$$
$$\left. + \frac{2}{3}(2\kappa - 1)I^+_{+-}\right],$$
$$G_M^{\text{BH}} = \frac{2}{2P^+(1+2\kappa)}\left[I^+_{00} + \frac{(2\kappa-1)}{\sqrt{2\kappa}}I^+_{+0} - I^+_{+-}\right], \qquad (7)$$
$$G_Q^{\text{BH}} = \frac{-1}{2P^+(1+2\kappa)}\left[I^+_{00} - 2\frac{I^+_{+0}}{\sqrt{2\kappa}} + \frac{1+\kappa}{\kappa}I^+_{+-}\right].$$

Of course, the matrix elements must fulfill the angular condition given by Eq. (4) for the physical form factors to be independent from the prescriptions (GK or BH).

At zero momentum transfer, these form factors are proportional to the usual static quantities of charge e, magnetic moment μ, and quadrupole moment Q [18,28]:

$$eG_C(0) = e, \qquad eG_M(0) = 2M_v\mu,$$
$$-eG_Q(0) = M_v^2 Q. \qquad (8)$$

For the general discussion of the high Q^2 behaviors in the spin-1 system, one may also define the structure functions $A(Q^2)$, $B(Q^2)$, and the tensor polarization T_{20} [27] through the relation to the physical form factors:

$$A(Q^2) = G_C^2 + \frac{2}{3}\kappa G_M^2 + \frac{8}{9}\kappa^2 G_Q^2, \qquad B(Q^2) = \frac{4}{3}\kappa(1+\kappa)G_M^2,$$
$$T_{20}(Q^2, \theta) = -\kappa\frac{\sqrt{2}}{3}\frac{\frac{4}{3}\kappa G_Q^2 + 4G_Q G_C + [1/2 + (1+\kappa)\tan^2(\theta/2)]G_M^2}{A + B\tan^2(\theta/2)}. \qquad (9)$$

We use this relation Eq. (9) in Sec. IV to numerically verify the recent discussion [30] on the non-negligible subleading contribution at the large Q^2 region as a consequence from the spin-1 angular condition.

III. MODEL DESCRIPTION AND CALCULATION

As we have shown in our previous work [6], the form factors of a spin-1 particle can be derived from the covariant Bethe-Salpeter model of $(3 + 1)$-dimensional fermion field theory.

The covariant diagram shown in Fig. 1(a) is in general equivalent to the sum of the LF valence diagram (b) and the nonvalence diagram (c), where $\alpha = P'^+/P^+ = 1 + q^+/P^+$. From the covariant diagram of Fig. 1(a), the electromagnetic current $I^\mu_{h'h}(0)$ of a spin-1 particle with equal constituent masses ($m = m_q = m_{\bar{q}}$) is given by

$$I^\mu_{h'h}(0) = iN_c g^2 \int \frac{d^4k}{(2\pi)^4} \frac{S_\Lambda(k-P)S^\mu_{h'h}S_\Lambda(k-P')}{[(k-P)^2 - m^2 + i\varepsilon][k^2 - m^2 + i\varepsilon][(k-P')^2 - m^2 + i\varepsilon]}, \qquad (10)$$

where N_c is the number of colors and g is the normalization constant modulo the charge factor e_q which can be fixed by requiring the charge form factor to be unity at $q^2 = 0$. In Ref. [6], we replaced the point photon vertex γ^μ by a nonlocal smeared photon vertex $S_\Lambda(P)\gamma^\mu S_\Lambda(P')$ to regularize the covariant fermion triangle loop in $(3 + 1)$ dimensions, where $S_\Lambda(P) = \Lambda^2/(P^2 - \Lambda^2 + i\varepsilon)$ and Λ plays the role of a momentum cutoff similar to the Pauli-Villars regularization. For the form factors calculated from this particular fermion loop, the results based on adopting a smeared photon vertex [6] are equivalent to those based on smearing the $q\bar{q}$ bound-state vertex, i.e., taking S_Λ as a part of the $q\bar{q}$ bound-state vertex rather than as a part of the photon vertex. However, there is a conceptual difference between these two choices of regularization because in principle the Bethe-Salpeter amplitude of the $q\bar{q}$ bound-state system should be distinct from the dressing of the photon vertex. Since the latter choice, i.e., smearing the $q\bar{q}$ bound-state vertex, leads naturally to the concept of a bound-state wave function in the valence sector, conceptually we are taking S_Λ in Eq. (10) as a part of $q\bar{q}$ bound-state vertex in this work. Since the replacement of the LF radial wave function by the one which has much more phenomenological support is considered later, such conceptual distinction in the choice of regularization is necessary at this point.
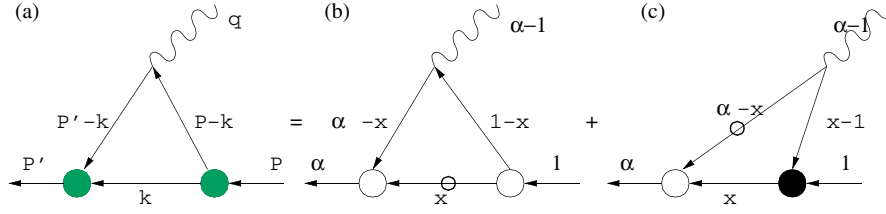
FIG. 1 (color online). Covariant triangle diagram (a) is represented as the sum of LF valence diagram (b) defined in the $0 < k^+ < P^+$ region and the nonvalence diagram (c) defined in the $P^+ < k^+ < P'^+$ region, where $\alpha = P'^+/P^+ = 1 + q^+/P^+$. The large white and black blobs at the meson-quark vertices in (b) and (c) represent the ordinary LF wave function and the nonvalence wave function vertices, respectively. The small white blobs in (b) and (c) represent the (on-shell) mass pole of the quark propagator determined from the k^- integration.

The trace term $S_{h'h}^\mu$ of the quark propagators in Eq. (10) is given by

$$S_{h'h}^\mu = (\epsilon_{h'}^*)_\alpha \mathrm{Tr}[\Gamma^\alpha(\not{p}' + m)\gamma^\mu(\not{p} + m)\Gamma^\beta(\not{k} + m)](\epsilon_h)_\beta,$$

(11)

where $p = k - P$, $p' = k - P'$, and $\Gamma^\beta(\Gamma^\alpha)$ is the spinor structure of the initial (final) state meson-quark vertex. In our previous work [6], using a rather simple meson vertex, $\Gamma^\mu = \gamma^\mu$, we showed that only S_{00}^+ receives zero-mode contributions.

The purpose of the present work is to go beyond the simple vertex, $\Gamma^\mu = \gamma^\mu$, and analyze the zero-mode contribution to see if the same conclusion (i.e., zero mode only in S_{00}^+) can be drawn. For this purpose, we extend the meson vertex to the more general one, which has been used for the phenomenology:

$$\Gamma^\beta = \gamma^\beta - \frac{(2k - P)^\beta}{D}, \quad \Gamma^\alpha = \gamma^\alpha - \frac{(2k - P')^\alpha}{D'}. \quad (12)$$

While in the manifestly covariant model, D and D' may be written as [32,33][1]

$$D_{\mathrm{cov}} = \frac{2}{M_v}(k \cdot P + M_v m - i\epsilon),$$
$$D'_{\mathrm{cov}} = \frac{2}{M_v}(k \cdot P' + M_v m - i\epsilon),$$

(13)

in the standard LFQM they are given by [3,8,18]

$$D_{\mathrm{LFQM}} = \sqrt{\frac{m^2 + \mathbf{k}_{i\perp}^2}{x(1 - x)}} + 2m = M_{0i} + 2m,$$
$$D'_{\mathrm{LFQM}} = \sqrt{\frac{m^2 + \mathbf{k}_{f\perp}^2}{x'(1 - x')}} + 2m = M_{0f} + 2m,$$

(14)

———

[1]In a brief presentation of Ref. [33], the authors indicated that they investigated the ρ meson form factors using Eq. (13). However, the detailed explicit calculations have not yet been presented. Moreover, the result shown in Ref. [33] was based on the instant-form polarization rather than the light-front polarization so that the direct analysis of light-front helicity amplitudes as discussed in this work has not yet been presented.

where $x' = x/\alpha$, $\alpha = P'^+/P^+ = 1 + q^+/P^+$ (i.e., $x' = x$ in the $q^+ = 0$ frame) and

$$\mathbf{k}_{i\perp} = \mathbf{k}_\perp + \frac{x}{2}\mathbf{q}_\perp, \qquad \mathbf{k}_{f\perp} = \mathbf{k}_\perp - \frac{x'}{2}\mathbf{q}_\perp. \quad (15)$$

We note that the LF meson vertex [Eq. (12)] with D_{LFQM} given by Eq. (14) can be obtained by the standard LF Melosh transformation [16]. The equivalence between $D_{\mathrm{cov}}(D'_{\mathrm{cov}})$ in Eq. (13) and $D_{\mathrm{LFQM}}(D'_{\mathrm{LFQM}})$ in Eq. (14) can be established only in a very limited case, e.g., zero-binding-energy limit, $M_v = M_0$.

As we have shown in our previous analysis, with a rather simple but manifestly covariant meson vertex ($\Gamma^\mu = \gamma^\mu$) [6,9], we can in principle duplicate both the manifestly covariant calculation and the LF calculation to check which form factors are immune to the zero mode. However, as we have also shown in Refs. [6,9], we can directly check the power counting of the longitudinal momentum fraction in the trace term to find out explicitly which helicity amplitude has the zero-mode contribution. No matter which way we check, the results are the same. In this work, we follow the latter procedure to check each helicity amplitude and show explicitly that both phenomenologically accessible meson vertices given by Eqs. (13) and (14) lead to the same conclusion, i.e., the zero-mode contribution exists only in the helicity zero-to-zero amplitude.

Before we proceed, we first summarize our result of the trace term for the "+" component of the current. Then, we separate the valence contribution from the nonvalence contribution and take the $q^+ \to 0$ limit of the nonvalence contribution to analyze the zero mode in each helicity amplitude.

A. Trace calculation

From Eqs. (11) and (12), we obtain the trace term for the + component of the current as follows:

$$S^+_{h'h} = (\epsilon^*_{h'})_\alpha \text{Tr}[\Gamma^\alpha(\not{p}' + m)\gamma^+(\not{p} + m)\Gamma^\beta(\not{k} + m)](\epsilon_h)_\beta,$$

$$= \text{Tr}[\not{\epsilon}^*_{h'}(\not{p}' + m)\gamma^+(\not{p} + m)\not{\epsilon}_h(\not{k} + m)] - \frac{\epsilon_h \cdot (2k - P)}{D}\text{Tr}[\not{\epsilon}^*_{h'}(\not{p}' + m)\gamma^+(\not{p} + m)$$

$$\times (\not{k} + m)], -\frac{\epsilon^*_{h'} \cdot (2k - P')}{D'}\text{Tr}[(\not{p}' + m)\gamma^+(\not{p} + m)\not{\epsilon}_h(k + m)],$$

$$+ \frac{\epsilon^*_{h'} \cdot (2k - P')}{D'} \frac{\epsilon_h \cdot (2k - P)}{D}\text{Tr}[(\not{p}' + m)\gamma^+(\not{p} + m)(\not{k} + m)],$$

$$= S^+_{1h'h} - S^+_{2h'h} - S^+_{3h'h} + S^+_{4h'h}. \tag{16}$$

Using the following identity:

$$\not{p} + m = (\not{p}_{\text{on}} + m) + \tfrac{1}{2}\gamma^+(p^- - p^-_{\text{on}}), \tag{17}$$

we separate the trace part for each $S^+_{ih'h}(i = 1, 2, 3, 4)$ into the on-mass shell [i.e., $p^2 = m^2$ or $p^- = p^-_{\text{on}} = (m^2 + \mathbf{p}^2_\perp)/p^+$] propagating part, $(S^+_{ih'h})_{\text{on}}$, and the off-shell part, $(S^+_{ih'h})_{\text{off}}$, i.e., $S^+_{ih'h} = (S^+_{ih'h})_{\text{on}} + (S^+_{ih'h})_{\text{off}}$. In the Appendix, we present the explicit expressions of $(S^+_{ih'h})$ in terms of LF variables.

Now, by doing the integration over k^- in Eq. (10), one finds the two LF time-ordered contributions to the residues corresponding to the two poles in k^-, the one coming from the interval (I) $0 < k^+ < P^+$ [see Fig. 1(b), the "valence contribution"], and the other from (II) $P^+ < k^+ < P'^+$ [see Fig. 1(c), the "nonvalence contribution"].

B. Valence contribution

In the valence region of $0 < k^+ < P^+$ as shown in Fig. 1(b), the residue is at the pole of $k^- = k^-_{\text{on}} = [m^2 + \mathbf{k}^2_\perp - i\varepsilon]/k^+$ (i.e., spectator quark), which is placed in the lower half of the complex-k^- plane. Thus, the Cauchy integration over k^- of the plus current, $I^+_{h'h}(0)$ [see Eq. (10)], in the Breit frame given by Eq. (2) yields

$$I^{+\text{val}}_{h'h} = \frac{N_c}{16\pi^3} \int_0^1 \frac{dx}{x(1 - x)^2}$$
$$\times \int d^2\mathbf{k}_\perp \chi_i(x, \mathbf{k}_{i\perp})S^+_{h'h}\chi_f(x, \mathbf{k}_{f\perp}), \tag{18}$$

where

$$\chi_i(x, \mathbf{k}_{i\perp}) = \frac{g\Lambda^2}{(1 - x)(M^2_v - M^2_{0i})(M^2_v - M^2_{\Lambda 0i})} \tag{19}$$

corresponds to the initial state meson vertex function with

$$M^2_{\Lambda 0i} = \frac{m^2 + \mathbf{k}^2_{i\perp}}{x} + \frac{\Lambda^2 + \mathbf{k}^2_{i\perp}}{1 - x}. \tag{20}$$

The final state denoted by subscript (f) can be obtained by replacing $(x, \mathbf{k}_{i\perp})$ with $(x', \mathbf{k}_{f\perp})$ in Eqs. (19) and (20). Since $k^- = k^-_{\text{on}}$ in the valence region, $(S^+_{h'h})_{\text{off}} = 0$ and $S^+_{h'h} = (S^+_{h'h})_{\text{on}}$.

C. Nonvalence contribution and zero mode in $q^+ \to 0$ limit

In the region $P^+ < k^+ < P'^+(= P^+ + q^+)$ as shown in Fig. 1(c), the poles are at $k^- \equiv k^-_m = P'^-_1 + [m^2 + (\mathbf{k}_\perp - \mathbf{P}'_\perp)^2 - i\varepsilon]/(k^+ - P'^+)$ (from the struck quark propagator) and $k^- \equiv k^-_\Lambda = P'^- + [\Lambda^2 + (\mathbf{k}^2_\perp - \mathbf{P}'_\perp)^2 - i\varepsilon]/(k^+ - P'^+)$ [from the smeared quark-photon vertex $S_\Lambda(k - P')$]. Both of them are located in the upper half of the complex k^- plane.

When we do the Cauchy integration over k^- to obtain the LF time-ordered diagrams, we decompose the product of five energy denominators in Eq. (10) into a sum of terms with three energy denominators [see Eq. (21) in Ref. [6]] to avoid the complexity of treating double k^- poles and obtain

$$I^{+nv}_{h'h} = -\frac{g^2\Lambda^4}{16\pi^3(\Lambda^2 - m^2)^2}\int_1^\alpha \frac{dx}{xx''(x - \alpha)}$$
$$\times \int d^2\mathbf{k}_\perp \left\{ \frac{S^+_{h'h}(k^- = k^-_\Lambda)}{(M^2_v - M^2_{0\Lambda f})(q^2 - M^2_{\Lambda\Lambda})} \right.$$
$$- \frac{S^+_{h'h}(k^- = k^-_\Lambda)}{(M^2_v - M^2_{0\Lambda f})(q^2 - M^2_{\Lambda m})}$$
$$+ \frac{S^+_{h'h}(k^- = k^-_m)}{(M^2_v - M^2_{0f})(q^2 - M^2_{mm})}$$
$$\left. - \frac{S^+_{h'h}(k^- = k^-_m)}{(M^2_v - M^2_{0f})(q^2 - M^2_{m\Lambda})} \right\}, \tag{21}$$

where

$$M^2_{\Lambda\Lambda} = \frac{\mathbf{k}''^2_\perp + \Lambda^2}{x''(1 - x'')}, \qquad M^2_{mm} = \frac{\mathbf{k}''^2_\perp + m^2}{x''(1 - x'')},$$
$$M^2_{\Lambda m} = \frac{\mathbf{k}''^2_\perp + \Lambda^2}{x''} + \frac{\mathbf{k}''^2_\perp + m^2}{1 - x''}, \tag{22}$$
$$M^2_{m\Lambda} = \frac{\mathbf{k}''^2_\perp + m^2}{x''} + \frac{\mathbf{k}''^2_\perp + \Lambda^2}{1 - x''},$$

with the variables defined by

$$x'' = \frac{1 - x}{1 - \alpha}, \qquad \mathbf{k}''_\perp = \mathbf{k}_\perp + \left(\frac{1}{2} - x''\right)\mathbf{q}_\perp. \tag{23}$$

Now, the zero mode [6] appears if the nonvalence diagram does not vanish in the $q^+ \to 0$ limit, i.e.,

$$\lim_{q^+\to 0}\int_{P^+}^{P^++q^+}dk^+(\cdots)\equiv\lim_{\alpha\to 1}\int_1^\alpha dx(\cdots)\neq 0. \quad (24)$$

To check if this is the case, we count the longitudinal momentum fraction factors in Eq. (21), e.g., in the $q^+\to 0$ limit, the first term in $I_{h'h}^{+\mu\nu}$ becomes

$$I_{h'h}^{+\text{z.m.}}\sim\lim_{\alpha\to 1}\int_1^\alpha\frac{dx}{xx''(x-\alpha)}\frac{S_{h'h}^+(k^-=k_\Lambda^-)}{(M_v^2-M_{0\Lambda f}^2)(q^2-M_{\Lambda\Lambda}^2)}$$

$$=\lim_{\alpha\to 1}\int_1^\alpha dx\frac{(1-x)}{(1-\alpha)}[\cdots]S_{h'h}^+(k_\Lambda^-), \quad (25)$$

where the factor $[\cdots]$ corresponds to the part that is regular as $q^+\to 0$ (i.e., $\alpha\to 1$). Thus, the nonvanishing zero-mode contribution is possible only if the longitudinal momentum fraction of $S_{h'h}^+(k^-)$ is proportional to $(1-x)^{-s}$ with $s\geq 1$. Otherwise, there is no zero-mode contribution since the integration range shrinks to zero as $q^+\to 0$. The other three terms in Eq. (21) have the same behavior as the first term shown.

Since we already know that the helicity zero-to-zero component, S_{00}^+, gives a nonvanishing zero-mode contribution at the level of a simple vertex, $\Gamma^+=\gamma^+$ [6], we need to focus on other helicity components for the vector meson vertex given by Eq. (12). In the nonvalence region $(P^+<k^+<P'^+)$, since the LF energy poles, k_m^- and k_Λ^-, are proportional to $k^-\sim 1/(1-x)$, we know that the D terms of covariant and LFQM vertices in Eq. (12) behave as

$$D_{\text{cov}}\sim\frac{1}{1-x},\qquad D_{\text{LFQM}}\sim\sqrt{\frac{1}{1-x}}, \quad (26)$$

by counting only the singular longitudinal momenta in the $\alpha\to 1$ (i.e., $x\to 1$) limit. We also note that the invariant mass in the D_{LFQM} for the initial state vector meson has to be replaced by

$$M_{0i}^2=\frac{m^2+\mathbf{k}_{i\perp}^2}{x}+\frac{m^2+\mathbf{k}_{i\perp}^2}{1-x}\to\frac{m^2+\mathbf{k}_{i\perp}^2}{x}+\frac{m^2+\mathbf{k}_{i\perp}^2}{x-1} \quad (27)$$

in the nonvalence region $(x>1)$ since the initial state vertex becomes the non-wave-function vertex [4] [see Fig. 1(c)]. Nevertheless, the power of the singular term in $1-x$ given in Eq. (26) remains the same. Now, from the explicit forms of the trace terms $S_{ih'h}^+$ given in the Appendix, we could determine the existence/nonexistence of the zero mode for each helicity component. Regardless of using covariant or LFQM vertices, we find that there are no singular terms in $1/(1-x)$ for the helicity $(++,+-,+0)$ components. The most problematic term regarding the zero mode was found to be the second term $(S_{2+0}^+)_{\text{off}}$ given by Eq. (A8), which is proportional to $(k^--k_{\text{on}}^-)/D$. While $(k^--k_{\text{on}}^-)/D_{\text{cov}}$ is regular in $1/(1-x)$, $(k^--k_{\text{on}}^-)/D_{\text{LFQM}}\sim\sqrt{1/(1-x)}$, i.e., S_{+0}^+

itself shows singular behavior in the $\alpha\to 1$ limit for the LFQM vertex. However, from Eq. (25), the net result of the zero-mode contribution to $I_{+0}^{+\text{z.m.}}$ for $D=D_{\text{LFQM}}$ is shown to be zero because

$$I_{+0}^{+\text{z.m.}}\sim\lim_{\alpha\to 1}\int_\alpha^1 dx\frac{(1-x)}{(1-\alpha)}[\cdots]\sqrt{\frac{1}{1-x}}=$$

$$\lim_{\alpha\to 1}\int_0^1 dz\frac{(1-\alpha)(1-z)}{\sqrt{(1-\alpha)(1-z)}}[\cdots]=0, \quad (28)$$

where the variable change $x=\alpha+(1-\alpha)z$ was made and the term $[\cdots]$ again corresponds to the regular part in the $q^+\to 0$ limit. For helicity (00) component, the zero-mode contribution comes from $(S_{100}^+)_{\text{off}}$ for both $D=D_{\text{cov}}$ and D_{LFQM} [see Eq. (A10)].

Thus, as in the case of Dirac coupling $\Gamma^\mu=\gamma^\mu$, we find that only I_{00}^+ receives the zero-mode contribution for the more general vertex structures given by Eq. (12) with D_{cov} and D_{LFQM}. Accordingly, we can compute the electromagnetic structure of the spin-1 particle using only the valence contribution as far as I_{00}^+ is avoided (e.g., GK prescription). Moreover, we may identify the zero-mode contribution to I_{00}^+ using the angular condition given by Eq. (4), i.e.,

$$I_{00}^{+\text{z.m.}}=(1+2\kappa)I_{++}^{+\text{val}}+I_{+-}^{+\text{val}}-\sqrt{8\kappa}I_{+0}^{+\text{val}}-I_{00}^{+\text{val}}, \quad (29)$$

in the $q^+=0$ frame with the LF gauge $\epsilon_\pm^+=0$.

Thus far, we relied on the generalization of the meson vertex [Eq. (12)] while we kept the use of the smeared photon vertex as adopted in Ref. [6]. Although the spin-orbit part of the LFQM can be incorporated by this generalization, the radial part of the LF wave function given by Eq. (19) may serve only a semirealistic calculation of physical observables as discussed by others [8,34]. For the more realistic calculation, one may need to replace the LF radial wave function by the one which has much more phenomenological support. For this purpose, we may utilize the LFQM presented in Ref. [22], which has been quite successful in predicting various static properties of low lying hadrons. Comparing χ in Eq. (18) with our light-front wave function given by Ref. [22], we get

$$\chi_i(x,\mathbf{k}_{i\perp})=\sqrt{\frac{8\pi^3}{N_c}}\sqrt{\frac{\partial k_z}{\partial x}}\frac{[x(1-x)]^{1/2}}{M_{0i}}\phi(x,\mathbf{k}_{i\perp}), \quad (30)$$

where the Jacobian of the variable transformation $\mathbf{k}=(k_z,\mathbf{k}_\perp)\to(x,\mathbf{k}_\perp)$ is obtained as $\partial k_z/\partial x=M_{0i}/[4x(1-x)]$ and the radial wave function is given by

$$\phi(\mathbf{k}^2)=\sqrt{\frac{1}{\pi^{3/2}\beta^3}}\exp(-\mathbf{k}^2/2\beta^2), \quad (31)$$

which is normalized as

$$\int d^3k |\phi(\mathbf{k}^2)|^2 = \int_0^1 dx \int d^2\mathbf{k}_\perp \left(\frac{\partial k_z}{\partial x}\right) |\phi(x, \mathbf{k}_\perp)|^2 = 1.$$

(32)

It is important to note that the end-point singularities are under control with the phenomenological wave function given by Eqs. (30) and (31) that falls exponentially to mock nonperturbative effects. The prefactor to $\phi(x, \mathbf{k}_{i\perp})$ in Eq. (30) is proportional to $(1 - x)^{1/4}$ and thus also regular in the limit $x \to 1$. In the next section, we shall investigate the ρ-meson electromagnetic properties using this model. We should note that this replacement of the radial part of the LF wave function cannot alter our conclusion of the zero mode (i.e., only in S_{00}^+) because the use of Eq. (30) is limited just for the valence contribution.

In summary, the LFQM described above provides the calculation of physical form factors with just the valence contribution of $I_{h'h}^+$ except the component of $(h', h) = (0, 0)$, i.e.,

$$I_{h'h}^{+\mathrm{LFQM}} = \int_0^1 \frac{dx}{2(1 - x)} \int d^2\mathbf{k}_\perp \sqrt{\frac{\partial k_z}{\partial x}} \sqrt{\frac{\partial k_z'}{\partial x}}$$
$$\times \phi(x, \mathbf{k}_{i\perp}) \phi^*(x, \mathbf{k}_{f\perp}) \frac{(S_{h'h}^+)_{\mathrm{on}}}{M_{0i} M_{0f}}. \quad (33)$$

Thus, in the GK prescription where I_{00}^+ is not used, it is easy to verify $G_C^{\mathrm{GK}}(0) = I_{++}^{+\mathrm{LFQM}}/2P^+ = 1$ because at $Q = 0$, $M_{0i}^2 = M_{0f}^2 = M_0^2 = (m^2 + \mathbf{k}_\perp^2)/x(1 - x)$, $(S_{++}^+)_{\mathrm{on}} = 4P^+(1 - x)M_0^2$ from a straightforward evaluation using Eq. (A3) and $(S_{+-}^+)_{\mathrm{on}} = 0$ from Eq. (A5).

However, the BH prescription involves the I_{00}^+ component and $G_C^{\mathrm{BH}}(0) = I_{00}^{+\mathrm{LFQM}}/2P^+ \neq 1$ due to the zero-mode contribution. It has been shown in Ref. [35] that the additive model for the current operator of interacting constituents is consistent with the angular condition only for the first two terms of the expansion of the plus (good) current in powers of the momentum transfer Q. Indeed, we can show that the zero-mode contribution to $I_{00}^{+\mathrm{LFQM}}$ vanishes in the zero-binding limit (i.e., $M_\nu = M_0$) and the angular condition $\Delta(0) = 0$ in this case. At the same token, we can show that $I_{++}^{+\mathrm{LFQM}} = I_{00}^{+\mathrm{LFQM}}$ [i.e., $(S_{++}^+)_{\mathrm{on}} = (S_{00}^+)_{\mathrm{on}}$ from Eqs. (A3) and (A9)] at $Q = 0$ in the zero-binding limit. In most previous LFQM analyses [16,18,36], the authors used not only the meson vertex factor given by Eq. (12) together with Eq. (14) but also the zero-binding-energy prescription, i.e., $M_\nu = M_0$, which is equivalent to replace M_ν in $\epsilon^\mu(P, 0)[\epsilon^\mu(P', 0)]$ with $M_{0i}[M_{0f}]$. In that case, the angular condition is zero at $Q^2 = 0$. However, in this work, we showed an explicit example which gives $\Delta(0) \neq 0$ even if the plus current is used. In Ref. [6], $\Delta(0) \neq 0$ was also shown. Thus, the zero-mode contribution is in general necessary even at $Q^2 = 0$ for the I_{00}^+ amplitude.

IV. NUMERICAL RESULTS

The model parameters used in our analysis are $m = 0.22$ GeV and $\beta = 0.3659$ GeV, which were obtained from the linear confining potential of our QCD-motivated effective Hamiltonian in LFQM [22], as well as $M_\nu = 0.77$ GeV.

First, we show in Fig. 2 the angular condition $\Delta(Q^2)$ given by Eq. (4) or Eq. (29) in the Breit frame defined by Eq. (2). In this particular reference frame, $\Delta(Q^2)$ is equal to the zero mode from the helicity zero-to-zero component, $I_{00}^{+\mathrm{z.m.}}$ in Eq. (29). Note that $\Delta(Q^2) \neq 0$ even at $Q^2 = 0$ (see the discussion just before this section). Unless the binding-energy zero limit ($M_\nu = M_0$) is taken, I_{00}^+ is not immune to the zero mode even at $Q^2 = 0$, but it eventually goes to zero as Q^2 becomes very large.

In Fig. 3, we plot the physical form factors, G_C, G_M, and G_Q, respectively. The solid lines represent the full solutions, i.e., the GK prescription in Eq. (6) or equivalently the BH prescription in Eq. (7) including the zero-mode contribution to I_{00}^+, i.e., $I_{00}^{+\mathrm{full}} = I_{00}^{+\mathrm{val}} + I_{00}^{+\mathrm{z.m.}}$, where $I_{00}^{+\mathrm{z.m.}}$ is obtained from Eq. (29). As they should be, the full solutions are found to be independent from the choice of prescription. The dashed lines represent the valence contributions to the form factors in the BH prescription. The dash-dotted lines represent the zero mode from the helicity zero-to-zero component, which turns out to be exactly the same with the difference between the solid and the dashed lines. For the charge form factor, $G_C(Q^2)$, we found it has a zero around $Q^2 = 5.5$ GeV^2,
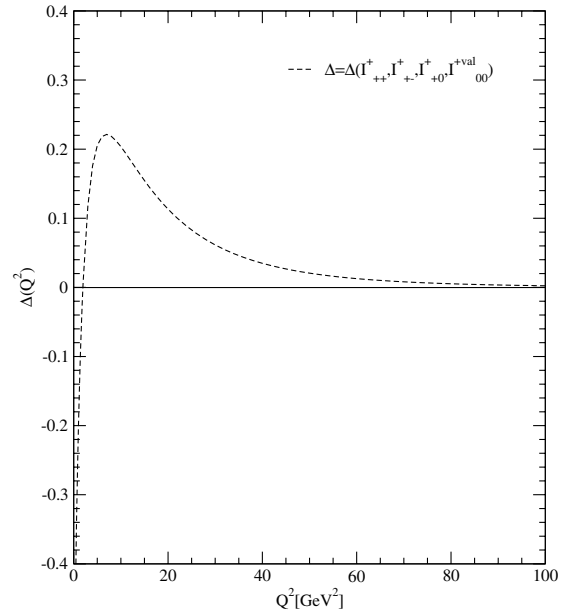
FIG. 2. The angular condition given by Eqs. (4) or (29) in the Breit frame, i.e., $\Delta(Q^2) = I_{00}^{+\mathrm{zm}}$. Note that the zero-mode contribution is necessary to satisfy the angular condition even at $Q^2 = 0$, where $\Delta(0) = -0.65$ in our model calculation.
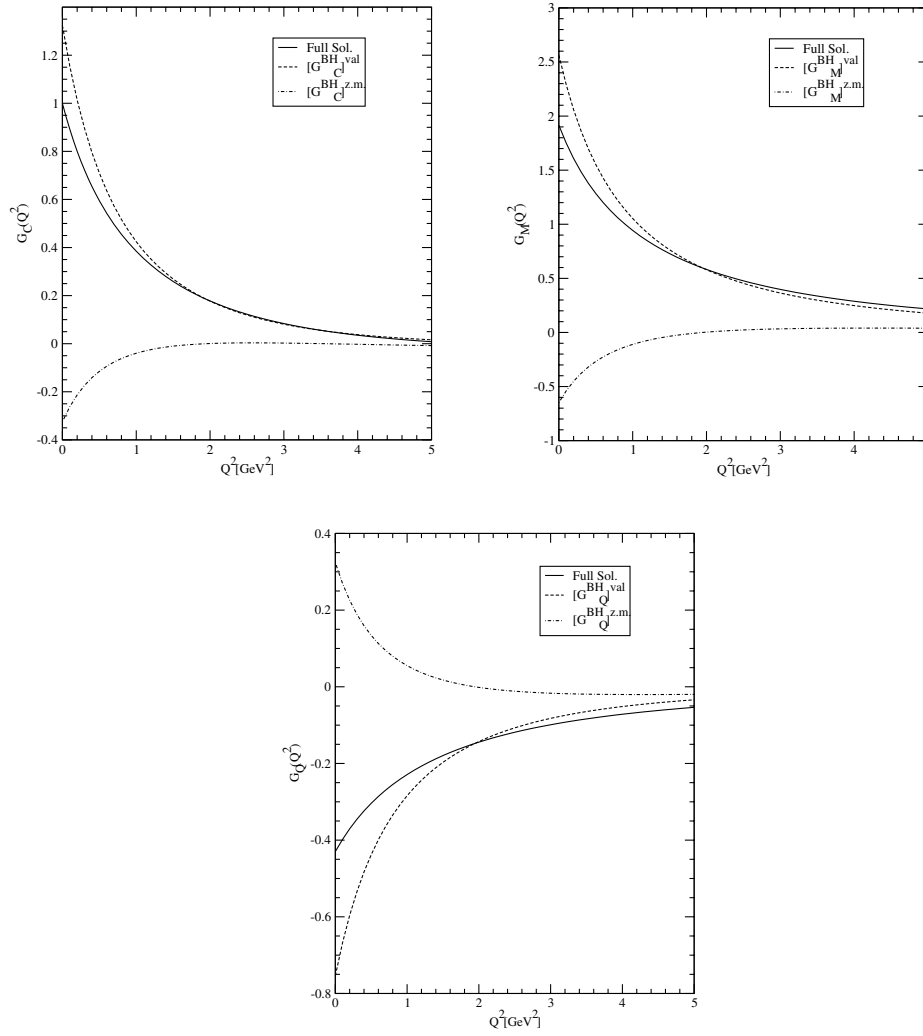
FIG. 3. Form factors of the ρ meson, i.e., charge [$G_C(Q^2)$], magnetic [$G_M(Q^2)$], and quadrupole [$G_Q(Q^2)$] form factors. The solid and dashed lines represent the full (i.e., valence + zero mode) solution and valence contribution ($I_{00}^{+\text{val}}$) to the form factors, respectively. The dash-dotted line represents the zero-mode contribution, i.e., full solution − valence contribution.

which is not shown in the figure. Also, the nonvanishing zero-mode contribution to I_{00}^+ at $Q^2 = 0$ is apparent in Fig. 3.

We also obtain the magnetic (in units of $e/2M_v$) and quadrupole (in units of e/M_v^2) moments for the ρ meson as

$$\mu = 1.92, \qquad Q = 0.43.$$

Our result for the magnetic moment without involving the zero mode is comparable to $\mu = 1.83$ in Ref. [8] and the one in Ref. [37], in which the author found $\mu < 2$ by considering the low energy limit of the radiative amplitudes in conjunction with the amplitude calculated by the hard-pion technique. The recent light-cone QCD sum rule [38] and the traditional QCD sum rule [39] reported $\mu = 2.3 \pm 0.5$ and 2.0 ± 0.3, respectively. We note that the author of Ref. [39] also preferred $\mu < 2$. On the other

hand, the previous LFQM [18,36] and the Dyson-Schwinger model [40,41] predicted $\mu > 2$. We summarize in Table I our results of magnetic dipole (μ) and quadrupole (Q) moments compared with other theoretical predictions.

Since it is difficult to have the ρ meson as a target, the definition of $A(Q^2)$, $B(Q^2)$, and $T_{20}(Q^2)$ is given only by the relation to the physical form factors as shown in Eq. (9). Nevertheless, the general discussion on the high

TABLE I. Magnetic dipole (μ) and quadrupole (Q) moments in units of $e/2M_v$ and e/M_v^2, respectively.

References	This work	[8]	[42]	[39]
μ	1.92	1.83	2.3	2.0 ± 0.3
Q	0.43	0.33	0.45	$\cdots$

Q^2 behaviors of $A(Q^2)$, $B(Q^2)$, and $T_{20}(Q^2)$ is still important because the subleading contribution in the deuteron case would be even greater than the ρ meson case. The subleading contribution as a consequence of the spin-1 angular condition has been discussed recently in Ref. [30]. In Fig. 4, we plot the structure functions $A(Q^2)$, $B(Q^2)$, and their ratio $\log_{10}(B/A)$ up to $Q^2 = 10$ GeV^2. The solid and dashed lines represent the full results and the contributions only from the $I_{00}^{+\text{full}}(= I_{00}^{+\text{val}} + I_{00}^{+\text{z.m.}})$ component, respectively. The dominance of helicity zero-to-zero amplitude at high Q^2 region [27,30,43] has been discussed in the context of PQCD counting rules and the naturalness condition [44]. However, the analysis of the angular condition [30] reveals that the subleading contributions $I_{+0}^{+} \sim (\Lambda_{\text{QCD}}/Q)I_{00}^{+}$ and $I_{++}^{+} \sim I_{+-}^{+} \sim (\Lambda_{\text{QCD}}/Q)^2 I_{00}^{+}$ are not as negligible as one might naively expect from PQCD. Our

LFQM results indicate that the dominance of I_{00}^{+} is realized in $A(Q^2)$ but not in $B(Q^2)$ [or $\log_{10}(B/A)$], supporting the significance of the subleading contribution discussed in Ref. [30]. For the magnetic form factor $G_M(Q^2)$ in Eq. (7), both I_{00}^{+} and I_{+0}^{+} terms contribute at the same order and the I_{+0}^{+} contribution at large Q^2 region (even at $Q^2 \sim 100$ GeV^2) is not negligible. This explains why we have discrepancies between the full results and I_{00}^{+} dominances for the calculations of $B(Q^2)$ and $\log_{10}(B/A)$.

In Fig. 5, we show the full solution of the tensor polarization $T_{20}(Q^2)$ at $\theta = 20°$ (dashed line) and at $\theta = 70°$ (solid line), respectively. For comparison, we also plot the $I_{00}^{+\text{full}}$ contribution to $T_{20}(Q^2)$ at $\theta = 20°$ (dot-dashed line) and at $\theta = 70°$ (dotted line), respectively. The $T_{20}(Q^2)$ results also indicate the non-negligible subleading contribution [30] even at a rather large Q^2 region.
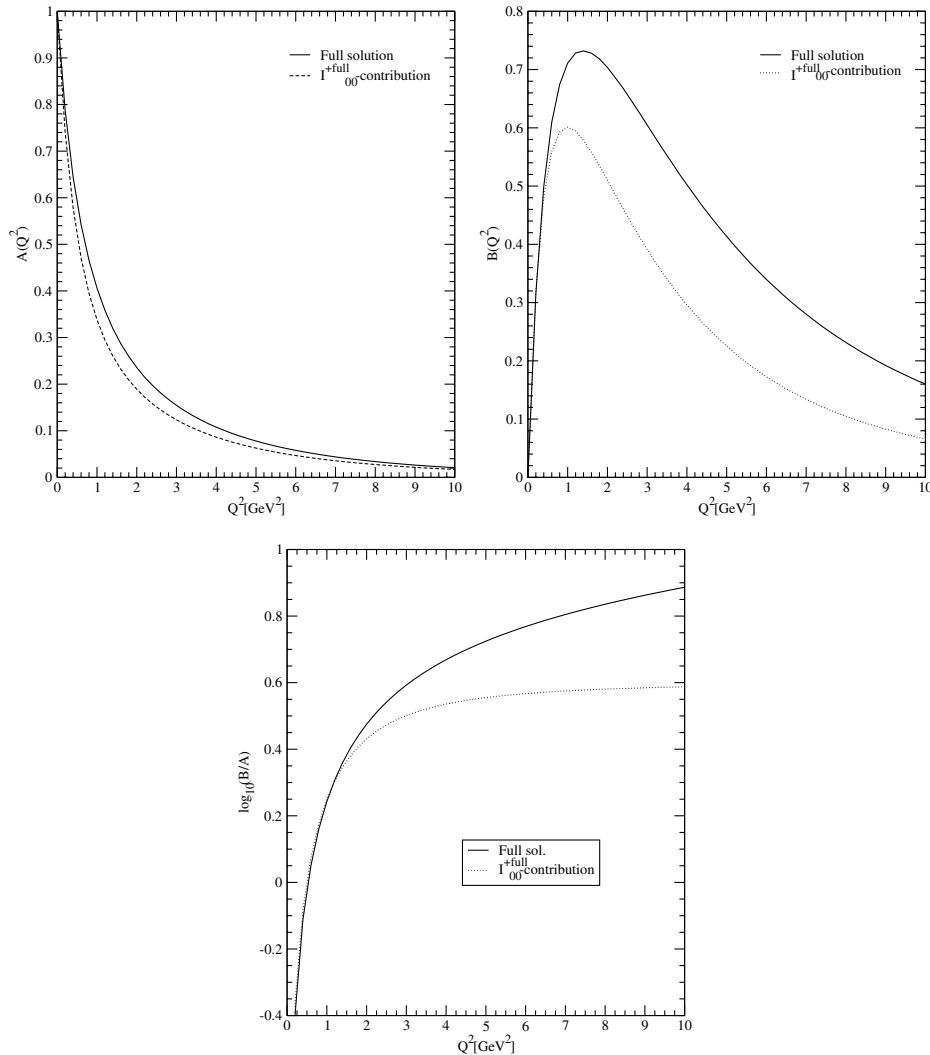

FIG. 4. Structure functions $A(Q^2)$, $B(Q^2)$, and their ratio $\log_{10}(B/A)$. Solid and dotted lines represent the full results and the contributions only from the $I_{00}^{+\text{full}} = I^{+\text{val}} + I^{+\text{z.m.}}$ component.
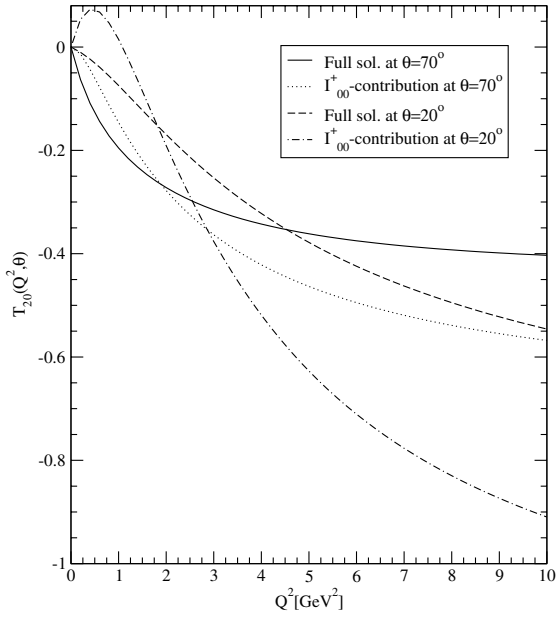
FIG. 5. Tensor polarization $T_{20}(Q^2)$ at $\theta = 70°$ (solid line) and $\theta = 20°$ (dashed line). For comparison, we also show the I_{00}^+ dominance at $\theta = 70°$ (dotted line) and $\theta = 20°$ (dot-dashed line).

V. CONCLUSION

In this work, we investigated the electromagnetic structure of the ρ meson in the light-front quark model. The two vector meson vertices are analyzed, i.e., the manifestly covariant vertex $D = D_{\text{cov}}$ and the LFQM vertex $D = D_{\text{LFQM}}$ consistent with the Melosh transformation. Using the power counting method for each helicity amplitude, we found that only the helicity zero-to-zero amplitude receives the zero-mode contribution regardless of $D = D_{\text{cov}}$ or $D = D_{\text{LFQM}}$. Other helicity amplitudes such as $(h', h) = (+, +)$, $(+, -)$, and $(+, 0)$ are found to be immune to the zero mode for both vertices. Much earlier than the present work, Ref. [32] presented the covariant calculation supporting the GK prescription with an effort to point out the role of the nonvalence contribution in

LFD. In this regard, Refs. [12,32] are quite relevant to the investigation of this paper. However, our finding is different from that in Ref. [8], in which the author found the nonvanishing zero-mode contribution to the helicity zero-to-plus component as well. This is significant because the absence of the zero-mode contribution in I_{+0}^+ allows that the pure valence contribution in LFD can give the full result of the physical form factors.

Further, we identified the zero-mode contribution to I_{00}^+ using the angular condition given by Eq. (29). Our result of $\Delta(Q^2)$ exhibits the nonvanishing zero mode even at $Q^2 = 0$ unless the binding-energy zero limit ($M_\nu = M_0$) is taken. This does not contradict the findings in the additive model for the current operator of interacting constituents discussed in Ref. [35]. Indeed, our calculations with $D = D_{\text{LFQM}}$ for $(h', h) = (+, +)$ and $(+, -)$ are equivalent to the previous LFQM [18,36] calculations based on the Melosh transformation. However, our calculations involving the helicity zero polarization vector, e.g., $(h', h) = (+, 0)$, cannot be the same with the previous Melosh-based calculations [18,36] unless the zero-binding limit $M_\nu = M_0$ is taken. One should note that the helicity zero polarization vector involves $1/M_\nu$ as a normalization factor [see Eq. (3)]. Thus, it appears important to analyze the difference in the physical observables including the binding-energy effects. As we presented in this work, our phenomenological LFQM prediction including the binding-energy effect (i.e., $M_\nu \neq M_0$) leads to $\mu = 1.92 < 2$, which is rather different from the previous results ($\mu > 2$) based on the free Melosh transformation [18,36,42].

Finally, our numerical results on $B(Q^2)$ and $T_{20}(Q^2)$ at the large Q^2 region support the significance of the subleading contribution, e.g., I_{+0}^+ contribution in $B(Q^2)$, found from the analysis of the angular condition in Ref. [30].

APPENDIX: SUMMARY OF TRACE TERMS IN HELICITY AMPLITUDES

The on-mass shell parts $(S_{ih'h}^+)_{\text{on}}$ in Eq. (16) are given by

$$(S_{1h'h}^+)_{\text{on}} = \text{Tr}[\not{\epsilon}_{h'}^*(\not{p}'_{\text{on}} + m)\gamma^+(\not{p}_{\text{on}} + m)\not{\epsilon}_h(\not{k}_{\text{on}} + m)],$$

$$(S_{2h'h}^+)_{\text{on}} = \frac{\epsilon_h \cdot (2k_{\text{on}} - P)}{D} \text{Tr}[\not{\epsilon}_{h'}^*(\not{p}'_{\text{on}} + m)\gamma^+(\not{p}_{\text{on}} + m)(\not{k}_{\text{on}} + m)],$$

$$(S_{3h'h}^+)_{\text{on}} = \frac{\epsilon_{h'}^* \cdot (2k_{\text{on}} - P')}{D'} \text{Tr}[(\not{p}'_{\text{on}} + m)\gamma^+(\not{p}_{\text{on}} + m)\not{\epsilon}_h(\not{k}_{\text{on}} + m)],$$

$$(S_{4h'h}^+)_{\text{on}} = \frac{\epsilon_{h'}^* \cdot (2k_{\text{on}} - P')}{D'} \frac{\epsilon_h \cdot (2k_{\text{on}} - P)}{D} \text{Tr}[(\not{p}'_{\text{on}} + m)\gamma^+(\not{p}_{\text{on}} + m)(\not{k}_{\text{on}} + m)],$$

$$(A1)$$

and the off-shell parts $(S_{ih'h}^+)_{\text{off}}$ in Eq. (16) are given by

$$(S_{1h'h}^+)_{\text{off}} = \frac{(k^- - k_{\text{on}}^-)}{2}\text{Tr}[\not\epsilon_{h'}^*(\not p'_{\text{on}} + m)\gamma^+(\not p_{\text{on}} + m)\not\epsilon_h\gamma^+],$$

$$(S_{2h'h}^+)_{\text{off}} = \frac{\epsilon_h^+(k^- - k_{\text{on}}^-)}{D}\text{Tr}[\not\epsilon_{h'}^*(\not p'_{\text{on}} + m)\gamma^+(\not p_{\text{on}} + m)(\not k_{\text{on}} + m)]$$

$$+ \frac{(k^- - k_{\text{on}}^-)}{2D}\epsilon_h \cdot (2k - P)\text{Tr}[\not\epsilon_{h'}^*(\not p'_{\text{on}} + m)\gamma^+(\not p_{\text{on}} + m)\gamma^+],$$

$$(S_{3h'h}^+)_{\text{off}} = \frac{\epsilon_{h'}^{*+}(k^- - k_{\text{on}}^-)}{D'}\text{Tr}[(\not p'_{\text{on}} + m)\gamma^+(\not p_{\text{on}} + m)\not\epsilon_h(\not k_{\text{on}} + m)] \qquad (A2)$$

$$+ \frac{(k^- - k_{\text{on}}^-)}{2D'}\epsilon_{h'}^* \cdot (2k - P')\text{Tr}[(\not p'_{\text{on}} + m)\gamma^+(\not p_{\text{on}} + m)\not\epsilon_h\gamma^+],$$

$$(S_{4h'h}^+)_{\text{off}} = \frac{(k^- - k_{\text{on}}^-)}{DD'}[\epsilon_h^+\epsilon_{h'}^* \cdot (2k_{\text{on}} - P') + \epsilon_{h'}^{*+}\epsilon_h \cdot (2k_{\text{on}} - P) + \epsilon_h^+\epsilon_{h'}^{*+}(k^- - k_{\text{on}}^-)]\text{Tr}[(\not p'_{\text{on}} + m)\gamma^+(\not p_{\text{on}} + m)$$

$$\times (\not k_{\text{on}} + m)] + \frac{(k^- - k_{\text{on}}^-)}{2DD'}\epsilon_{h'}^* \cdot (2k - P')\epsilon_h \cdot (2k - P)\text{Tr}[(\not p'_{\text{on}} + m)\gamma^+(\not p_{\text{on}} + m)\gamma^+].$$

In the Breit frame with the LF gauge given by Eqs. (2) and (3), the explicit forms of the trace terms in Eqs. (A1) and (A2) for each helicity component are given as follows.

(I) helicity (+ +) component:

$$(S_{1++}^+)_{\text{on}} = \frac{4P^+}{x}\left[m^2 + (2x^2 - 2x + 1)\left(\mathbf{k}_\perp^2 - \frac{x^2}{4}Q^2 - ixk_yQ\right)\right],$$

$$(S_{2++}^+)_{\text{on}} = -2P^+\left(\frac{m}{D}\right)[8(1 - x)\mathbf{k}_\perp^2 + x(2x^2 - 2x + 1)Q^2 + 2k_xQ + 2ik_yQ(2x - 1)^2],$$

$$(S_{3++}^+)_{\text{on}} = -2P^+\left(\frac{m}{D'}\right)[8(1 - x)\mathbf{k}_\perp^2 + x(2x^2 - 2x + 1)Q^2 - 2k_xQ + 2ik_yQ(2x - 1)^2], \qquad (A3)$$

$$(S_{4++}^+)_{\text{on}} = \frac{4P^+}{DD'}\left[\mathbf{k}_\perp^2 - \frac{x^2}{4}Q^2 - ixk_yQ\right][(1 - x)(M_{0i}^2 + M_{0f}^2 - 8m^2) - xQ^2],$$

and

$$(S_{1++}^+)_{\text{off}} = 4(P^+)^2(k^- - k_{\text{on}}^-)(1 - x)^2, \qquad (S_{2++}^+)_{\text{off}} = (S_{3++}^+)_{\text{off}} = 0,$$

$$(S_{4++}^+)_{\text{off}} = \frac{8(P^+)^2}{DD'}(1 - x)^2(k^- - k_{\text{on}}^-)\left[\mathbf{k}_\perp^2 - \frac{x^2}{4}Q^2 - ixk_yQ\right]. \qquad (A4)$$

In the nonvalence region where $k^- \sim 1/(1 - x)$, $D = D_{\text{cov}} \sim 1/(1 - x)$ and $D = D_{\text{LFQM}} \sim \sqrt{1/(1 - x)}$. Thus, we find from the power counting for the longitudinal momentum fraction that all the off-shell trace terms $(S_{i++}^+)_{\text{off}}$ ($i = 1, 2, 3, 4$) are regular as $q^+ \to 0$ (or equivalently $x \to 1$). Therefore, there is no zero mode in the helicity (+ +) component.

(II) helicity (+ −) component:

$$(S_{1+-}^+)_{\text{on}} = 2P^+(1 - x)[4(k^L)^2 - x^2Q^2],$$

$$(S_{2+-}^+)_{\text{on}} = 2P^+\left(\frac{m}{D}\right)(2k^L + xQ)[(2x^2 - 2x + 1)Q + 4(1 - x)k^L],$$

$$(S_{3+-}^+)_{\text{on}} = -2P^+\left(\frac{m}{D'}\right)(2k^L - xQ)[(2x^2 - 2x + 1)Q - 4(1 - x)k^L], \qquad (A5)$$

$$(S_{4+-}^+)_{\text{on}} = -\frac{P^+}{DD'}[4(k^L)^2 - x^2Q^2][(1 - x)(M_{0i}^2 + M_{0f}^2 - 8m^2) - xQ^2],$$

and

$$(S_{1+-}^+)_{\text{off}} = (S_{2+-}^+)_{\text{off}} = (S_{3+-}^+)_{\text{off}} = 0, \qquad (S_{4+-}^+)_{\text{off}} = -\frac{2(P^+)^2}{DD'}(k^- - k_{\text{on}}^-)(1-x)^2[4(k^L)^2 - x^2Q^2]. \qquad (A6)$$

Again, from the power counting for the longitudinal momentum fraction, $(S_{4+-}^+)_{\text{off}}$ is regular as $x \to 1$. Therefore, there is no zero mode in the helicity $(+-)$ component.

(III) helicity $(+0)$ component:

$$(S_{1+0}^+)_{\text{on}} = \frac{P^+\sqrt{2}}{M_v}(2k^L - xQ)(2x-1)(1-x)(M_{0i}^2 + M_v^2),$$

$$(S_{2+0}^+)_{\text{on}} = -\frac{4P^+}{M_v\sqrt{2}}\left(\frac{m}{D}\right)[(1-x)M_{0i}^2 - xM_v^2][(2x^2 - 2x + 1)Q + 4(1-x)k^L],$$

$$(S_{3+0}^+)_{\text{on}} = \frac{4P^+}{M_v\sqrt{2}}\left(\frac{m}{D'}\right)(2x-1)(1-x)(M_{0i}^2 + M_v^2)(2k^L - xQ), \qquad (A7)$$

$$(S_{4+0}^+)_{\text{on}} = \frac{P^+\sqrt{2}}{M_vDD'}(2k^L - xQ)[(1-x)M_{0i}^2 - xM_v^2][(1-x)(M_{0i}^2 + M_{0f}^2 - 8m^2) - xQ^2],$$

and

$$(S_{1+0}^+)_{\text{off}} = -\frac{4(P^+)^2}{M_v\sqrt{2}}(k^- - k_{\text{on}}^-)(1-x)(2k^L + xQ),$$

$$(S_{2+0}^+)_{\text{off}} = -\frac{4(P^+)^2}{M_v\sqrt{2}}\left(\frac{m}{D}\right)(k^- - k_{\text{on}}^-)[(2x^2 - 2x + 1)Q + 4(1-x)k^L],$$

$$(S_{3+0}^+)_{\text{off}} = -\frac{4(P^+)^2}{M_v\sqrt{2}}\left(\frac{m}{D'}\right)(k^- - k_{\text{on}}^-)(1-x)(2k^L - xQ), \qquad (A8)$$

$$(S_{4+0}^+)_{\text{off}} = \frac{(P^+)^2\sqrt{2}}{M_vDD'}(k^- - k_{\text{on}}^-)(2k^L - xQ)[(1-x)(M_{0i}^2 + M_{0f}^2 - 8m^2) - xQ^2]$$

$$+ \frac{2\sqrt{2}(P^+)^2}{M_vDD'}(k^- - k_{\text{on}}^-)(1-x)^2(2k^L - xQ)[(1-x)M_{0i}^2 - xM_v^2] + \frac{2\sqrt{2}(P^+)^3}{M_vDD'}(k^- - k_{\text{on}}^-)^2(1-x)^2(2k^L - xQ).$$

From the power counting of the longitudinal momentum fraction in the nonvalence region, we find only $(S_{2+0}^+)_{\text{off}}$ for $D = D_{\text{LFQM}}$ shows singular behavior, i.e., $(S_{2+0}^+)_{\text{off}} \sim \sqrt{1/(1-x)}$ as $x \to 1$. However, as we show in Eq. (28), the resulting zero-mode contribution vanishes due to the prefactor involved in the integration. Therefore, there is no zero-mode contribution to the helicity $(+0)$ component.

(IV) helicity (00) component:

$$(S_{100}^+)_{\text{on}} = \frac{4P^+}{M_v^2}x(1-x)^2(M_{0i}^2 + M_v^2)(M_{0f}^2 + M_v^2),$$

$$(S_{200}^+)_{\text{on}} = \frac{4P^+}{M_v^2}\left(\frac{m}{D}\right)(2x-1)(1-x)(M_{0f}^2 + M_v^2)[(1-x)M_{0i}^2 - xM_v^2],$$

$$(S_{300}^+)_{\text{on}} = \frac{4P^+}{M_v^2}\left(\frac{m}{D'}\right)(2x-1)(1-x)(M_{0i}^2 + M_v^2)[(1-x)M_{0f}^2 - xM_v^2], \qquad (A9)$$

$$(S_{400}^+)_{\text{on}} = \frac{2P^+}{M_v^2DD'}[(1-x)M_{0i}^2 - xM_v^2][(1-x)M_{0f}^2 - xM_v^2][(1-x)(M_{0i}^2 + M_{0f}^2 - 8m^2) - xQ^2],$$

and

$$(S_{100}^+)_{\text{off}} = \frac{4(P^+)^2}{M_v^2}(k^- - k_{\text{on}}^-)[m^2 + \mathbf{k}_\perp^2 - x^2 Q^2/4],$$

$$(S_{200}^+)_{\text{off}} = \frac{4(P^+)^2}{M_v^2}\left(\frac{m}{D}\right)(k^- - k_{\text{on}}^-)(1-x)(2x-1)(M_{0f}^2 + M_v^2)$$

$$- \frac{4(P^+)^2}{M_v^2}\left(\frac{m}{D}\right)(k^- - k_{\text{on}}^-)(1-x)[(1-x)M_{0i}^2 - xM_v^2 + (k^- - k_{\text{on}}^-)P^+],$$

$$(S_{300}^+)_{\text{off}} = \frac{4(P^+)^2}{M_v^2}\left(\frac{m}{D'}\right)(k^- - k_{\text{on}}^-)(1-x)(2x-1)(M_{0i}^2 + M_v^2) \tag{A10}$$

$$- \frac{4(P^+)^2}{M_v^2}\left(\frac{m}{D'}\right)(k^- - k_{\text{on}}^-)(1-x)[(1-x)M_{0f}^2 - xM_v^2 + (k^- - k_{\text{on}}^-)P^+],$$

$$(S_{400}^+)_{\text{off}} = \frac{2(P^+)^2}{M_v^2 DD'}(k^- - k_{\text{on}}^-)[(1-x)(M_{0i}^2 + M_{0f}^2) - 2xM_v^2][(1-x)(M_{0i}^2 + M_{0f}^2 - 8m^2) - xQ^2] + \frac{2(P^+)^3}{M_v^2 DD'}(k^- - k_{\text{on}}^-)^2$$

$$\times [(1-x)(M_{0i}^2 + M_{0f}^2 - 8m^2) - xQ^2] + \frac{4(P^+)^2}{M_v^2 DD'}(k^- - k_{\text{on}}^-)(1-x)^2\{[(1-x)M_{0i}^2 - xM_v^2][(1-x)$$

$$\times M_{0f}^2 - xM_v^2] + P^+(k^- - k_{\text{on}}^-)[(1-x)(M_{0i}^2 + M_{0f}^2) - 2xM_v^2] + (P^+)^2(k^- - k_{\text{on}}^-)^2\}.$$

From the power counting of the longitudinal momentum fraction, only $(S_{100}^+)_{\text{off}}$ is singular for both D_{cov} and D_{LFQM}, i.e., $(S_{100}^+)_{\text{off}} \sim 1/(1-x)$ as $x \to 1$, which gives the zero-mode contribution to the helicity zero-to-zero component.

[1] S. J. Brodsky, H. C. Pauli, and S. S. Pinsky, Phys. Rep. **301**, 299 (1998).
[2] J. Carbonell, B. Desplanques, V. A. Karmanov, and J.-F. Mathiot, Phys. Rep. **300**, 215 (1998).
[3] W. Jaus, Phys. Rev. D **60**, 054026 (1999).
[4] C.-R. Ji and H.-M. Choi, Phys. Lett. B **513**, 330 (2001); eConf C010430: T23, 2001.
[5] B. L. G. Bakker, H.-M. Choi, and C.-R. Ji, Phys. Rev. D **63**, 074014 (2001).
[6] B. L. G. Bakker, H.-M. Choi, and C.-R. Ji, Phys. Rev. D **65**, 116001 (2002).
[7] D. Melikhov and S. Simula, Phys. Rev. D **65**, 094043 (2002); S. Simula, Phys. Rev. C **66**, 035201 (2002).
[8] W. Jaus, Phys. Rev. D **67**, 094010 (2003).
[9] B. L. G. Bakker, H.-M. Choi, and C.-R. Ji, Phys. Rev. D **67**, 113007 (2003).
[10] S.-J. Chang and T.-M. Yan, Phys. Rev. D **7**, 1147 (1973); **7**, 1780 (1973).
[11] M. Burkardt, Nucl. Phys. **A504**, 762 (1989).
[12] J. P. B. C. de Melo, J. H. O. Sales, T. Frederico, and P. U. Sauer, Nucl. Phys. **A631**, 574c (1998); J. P. B. C. de Melo, T. Frederico, H. W. L. Naus, and P. U. Sauer, Nucl. Phys. **A660**, 219 (1999).
[13] S. J. Brodsky and D. S. Hwang, Nucl. Phys. **B543**, 239 (1998).
[14] H.-M. Choi and C.-R. Ji, Phys. Rev. D **58**, 071901 (1998).
[15] N. C. J. Schoonderwoerd and B. L. G. Bakker, Phys. Rev. D **57**, 4965 (1998); **58**, 025013 (1998).
[16] W. Jaus, Phys. Rev. D **41**, 3394 (1990); **44**, 2851 (1991).
[17] W. Jaus, Phys. Rev. D **53**, 1349 (1996); **54**, 5904(E) (1996).
[18] F. Cardarelli, I. L. Grach, I. M. Narodetskii, G. Salme, and S. Simula, Phys. Lett. B **349**, 393 (1995).
[19] D. Melikhov, Phys. Rev. D **53**, 2460 (1996); Phys. Lett. B **380**, 363 (1996).
[20] H.-M. Choi and C.-R. Ji, Nucl. Phys. **A618**, 291 (1997).
[21] H.-M. Choi and C.-R. Ji, Phys. Rev. D **56**, 6010 (1997).
[22] H.-M. Choi and C.-R. Ji, Phys. Rev. D **59**, 074015 (1999).
[23] W. Jaus (private communication).
[24] R. G. Arnold, C. E. Carlson, and F. Gross, Phys. Rev. C **21**, 1426 (1980).
[25] I. L. Grach and L. A. Kondratyuk, Sov. J. Nucl. Phys. **39**, 198 (1984).
[26] P. L. Chung, F. Coester, B. D. Keister, and W. N. Polyzou, Phys. Rev. C **37**, 2000 (1988).

[27] S. J. Brodsky and J. R. Hiller, Phys. Rev. D **46**, 2141 (1992).

[28] B. D. Keister, Phys. Rev. D **49**, 1500 (1994).

[29] J. D. Bjorken and S. D. Drell, *Relativistic Quantum Mechanics* (McGraw-Hill, New York, 1964); *Relativistic Quantum Fields* (McGraw-Hill, New York, 1965).

[30] Carl E. Carlson and C.-R. Ji, Phys. Rev. D **67**, 116002 (2003).

[31] V. A. Karmanov, Nucl. Phys. **A608**, 316 (1996).

[32] J. P. B. C. de Melo and T. Frederico, Phys. Rev. C **55**, 2043 (1997).

[33] J. P. B. C. de Melo and T. Frederico, hep-ph/0311079.

[34] T. Frederico and G. A. Miller, Phys. Rev. D **45**, 4207 (1992).

[35] L. A. Kondratyuk and M. Strikman, Nucl. Phys. **A426**, 575 (1984).

[36] D. Arndt and C.-R. Ji, Phys. Rev. D **60**, 094020 (1999).

[37] R. Shtokhamer and P. Singer, Phys. Rev. D **7**, 790 (1973).

[38] T. M. Aliev, I. Kanik, and M. Savci, Phys. Rev. D **68**, 056002 (2003).

[39] A. Samsonov, J. High Energy Phys. 12 (2003) 061.

[40] F. Hawes and M. Pichowsky, Phys. Rev. C **59**, 1743 (1999).

[41] M. Hecht and B. H. J. McKellar, Phys. Rev. C **57**, 2638 (1998).

[42] A. S. Bagdasaryan and S. V. Esaybegyan, Yad. Fiz. **42**, 440 (1985) [Sov. J. Nucl. Phys. **42**, 278 (1985)].

[43] Carl E. Carlson, J. Hiller, and R. Holt, Annu. Rev. Nucl. Part. Sci. **47**, 395 (1997).

[44] B. L. G. Bakker and C.-R. Ji, Phys. Rev. D **65**, 073002 (2002).